

# Combined use of 3D printing and computer-assisted navigation in the clinical treatment of multiple maxillofacial fractures

**Haohong Wang**

The First Affiliated Hospital of Anhui Medical University

**Yifan Chi**

The First Affiliated Hospital of Anhui Medical University

**Hanxiao Huang**

The First Affiliated Hospital of Anhui Medical University

**Shiheng Su**

The First Affiliated Hospital of Anhui Medical University

**Jun Hou** (✉ [2223409716@qq.com](mailto:2223409716@qq.com))

The First Affiliated Hospital of Anhui Medical University

**Haowei Xue**

The First Affiliated Hospital of Anhui Medical University

---

## Research Article

**Keywords:** multiple maxillofacial fractures, 3D-printed guide, CAN, three-dimensional reconstruction

**Posted Date:** February 25th, 2022

**DOI:** <https://doi.org/10.21203/rs.3.rs-1377915/v2>

**License:** © ⓘ This work is licensed under a Creative Commons Attribution 4.0 International License.

[Read Full License](#)

---

# Abstract

*Objectives:* Although computer-assisted navigation (CAN) has been widely used in the reconstruction of maxillofacial fractures, the direct guidance it provides for surgical operations and the handling of multiple maxillofacial fractures is insufficient due to the lack of a healthy side for reference. To address the above problems, a 3D-printed guide and head model was used in combination with CAN in this study.

*Materials and Methods:* In this process, 26 patients were randomly selected among those with multiple fractures treated from 09/2017 to 03/2021. They were randomly divided into the experimental and control groups, with 3D-printed guides and models used in the former group. The surgical time was compared between the groups, and posttreatment computed tomography and follow-up visits were conducted at 1 week and 3 months, respectively, to compare the quality of treatment in terms of infection, occlusal disorder, restricted mouth opening, midline displacement, and bilateral asymmetry. The Spearman rank correlation coefficient was used for assessment.

*Results:* According to our results, the therapeutic effect was excellent for 12 patients and satisfactory for 1 patient among the 13 patients in the experimental group, while the therapeutic effect was excellent in only 7, satisfactory in 3, and unsatisfactory in 3 patients in the control group.

*Conclusions:* According to our analysis, the combined use of CAN and 3D printing significantly improved the treatment results of double-sided maxillofacial fractures ( $r_s=0.448$ ,  $P<0.05$ ). The surgical time of the experimental group was significantly shorter than that of the control group ( $Z=-2.083$ ,  $P<0.05$ ).

*Clinical Relevance:* This study broadens our understanding of the treatment of multiple maxillofacial fractures. The combined use of 3D printing technology and CAN effectively shortened the operation time and achieved a better therapeutic effect.

## 1. Introduction

Multiple maxillofacial fractures have serious health consequences, including facial distortion, masticatory malfunction and impaired mouth-opening ability[1]. Since they are commonly caused by severe injuries from violence, falls and traffic accidents, important organs can be damaged at the same time[2]. These injuries are more life-threatening and need immediate treatment. As a result, multiple maxillofacial fractures are often treated after a delay, which results in inevitable deterioration over time and increases the difficulty of surgical operations[3]. As such, relatively high accuracy is needed in these operations.

Developments in digital technology have led to the increasingly widespread use of various types of guide plates in different fields of oral and maxillofacial surgery, including orthognathic and mandibular reconstruction and foreign body localization and removal, all of which have achieved good clinical results[4-7]. For patients with jaw fractures, anatomical reduction is required for the jaw to form a stable relationship with the surrounding muscles, to reduce muscle tension interference, to achieve a balance

between bone tissue and surrounding muscle tissue, and to reduce the probability of a poor postoperative occlusal relationship[8]. When performing solid internal fixation, it is necessary to ensure the stability of the reduction of the fractured end and select appropriate titanium plates and titanium screws according to the fracture condition[9]. Before using the titanium plate, it should be shaped to fit the bone surface as closely as possible and placed in a position with sufficient bone volume in the same direction as the stress and tension bands. Additionally, a sufficient number of titanium nails matching the titanium plate should be used.

In the treatment of complex fractures, it can be very difficult to quantify the standard of intraoperative reduction. Preoperative three-dimensional reconstruction technology can improve the appropriateness of the operation plan, and computer navigation technology can also accurately localize the intraoperative displacement of multiple bone fragments to a certain extent; nevertheless, precision therapy remains a difficult clinical challenge[10, 11]. For example, reconstruction can be directly achieved by mirror image technology and computer-assisted navigation (CAN). In multiple maxillofacial fractures, however, both the bilateral profile and occlusal relationship are damaged, making it infeasible to achieve reconstruction using symmetry. Therefore, reconstruction must be performed based on the personal experience of the operator, which is random, lacks accuracy, and may lead to unsatisfactory treatment results with complications[12, 13]. Additionally, the sole use of CAN is insufficient to provide straightforward guidance for fracture reduction, and it is difficult to optimize the surgical design, internal fixation, and surgical approach, which are key for successful treatment[14-17]. Due to the abovementioned limitations, CAN has rarely been reported in the treatment of multiple maxillofacial fractures.

These problems can potentially be solved with assistance from 3D printing technology. The insufficiency of CAN for reconstruction and surgical guidance can potentially be addressed by the use of 3D-printed head models and guides, respectively, allowing optimal precision and decision-making in the surgical operation.

In this study, 3D-printed guides and head models were used in combination with CAN for treating multiple maxillofacial fractures, and their effects on improving the treatment results were investigated. We believe the study will broaden our understanding of treatments for multiple maxillofacial fractures.

## **2. Materials And Methods**

Patients who underwent treatment for multiple complicated maxillofacial fractures in our department from September 2017 to March 2021 were included in the study. This study was approved by the medical ethics committee of the First Affiliated Hospital of Anhui Medical University (Quick-PJ 2021-10-27).

### **Study design**

A parallel group design was adopted in this RCT. Two groups were established: an experimental group (navigation-aided surgery combined with a 3D-printed guide) and a control group (navigation-aided surgery only). Participants were randomly assigned to each group at a 1:1 ratio. The investigators responsible for taking the measurements and conducting the statistical analysis were blinded to the group assignment. All surgeries were performed by the same experienced clinical surgeon team (Fig. 1).

## **Participants and sample size**

The inclusion criteria were as follows: 1. maxillofacial fractures involving both sides; 2. complete operative data; and 3. occlusal disorder.

The exclusion criteria were as follows: 1. facial shape and function affected without dysfunction; 2. incomplete operative data; 3. refusal to participate; and 4. loss to follow-up.

## **Interventions**

1. Acquisition of preoperative CT data: Spiral CT (Light Speed VCT, GE Co., Ltd) was used to obtain the patient's soft and hard tissue data, and the three-dimensional CT facial scan data was stored in the DICOM format.

2. Generation of 3D models (Fig. 1): The CT data was imported into Medical 3D Image Processing Software (Zhongjian 3DSCI-TECHCH. Ltd., Anhui, China) and processed according to clinical requirements to generate a digital 3D model. Fracture segments were defined and marked with different colors.

3. Virtual surgical planning (Fig. 2): Virtual surgeries were designed in Medical 3D Image Processing Software. According to the occlusal relationship and anatomical shape, the fractures were reconstructed by virtual surgery. The generated 3D images were imported into the AccuNavi-A navigation system (UEG Medical Devices Co., Ltd) as the surgical navigation planning scheme.

4. Design and manufacture of 3D printing guide plate and head mold (Fig. 3): The surgical guide was designed according to the occlusal relationship and jaw shape after virtual surgical reduction and manufactured by 3D printing using a digital light processing-based printer (Figure 4 Modular, 3D system). A titanium plate (Martin Medical Technical Development Co., Ltd.) was applied to the jaw model according to the virtual surgical scheme. The surgical guides and titanium plate were sterilized at low temperature for use during the operation.

5. Operation (Fig. 4): The operation was performed under general anesthesia. The reference frame and positioning ball were installed and fixed on the forehead of the patient. After the 3D-printed positioning guide was applied, the CAN probes were registered in sequence, and the actual position of the patient was

correlated with the navigation data to verify the registration accuracy. Then the broken ends of the bones were exposed, granulation tissue was scraped off from the fracture line, and the attached muscle was stripped to free the fracture fragments. The CAN probe was placed at the broken end of the fracture after reduction to judge the position relative to the preoperative plan. Under guidance of the 3D-printed guide, the fracture fragments were reconstructed. After fracture fragment reduction, the titanium plate was placed on the 3D-printed head die for forming, and the fracture fragments were fixed. Finally, the surgical area was flushed, hemostasis was achieved, and the surgical incision was closed. All patients underwent treatment with intermaxillary traction and antibiotics to prevent infection.

## Statistical method

The operation time was used as a statistical indicator and analyzed with the Wilcoxon rank-sum test.  $P < 0.05$  indicated statistical significance. Statistical analyses were conducted with SPSS 23.0 software (SPSS reference).

The patients were followed up 3 months after the operation to assess the results. Multiple key results were measured, including the symmetry of the patient's maxillofacial region and midline, the occurrence of infection in the operative area, the occlusal relationship, and mouth opening. The evaluation criteria were as follows:

1. Measurement of multiple key results, including the symmetry of the patient's maxillofacial region and the midline. The point of the eyebrow (G), the suborbital foramen [K (L, R)], and the midpoint of the zygomaticotemporal suture [Er (L, R)] were marked on the postoperative CT of each patient. Symmetry was judged based on the absolute value of the difference between the bilateral G-K values and G-Er values. If the absolute value was greater than 2 mm, the bilateral shape of the maxillofacial region was considered to be asymmetrical.
2. Infection in the operative area: The patient's white blood cell count was normal 3 days after surgery, there was no suppuration in the operation area and no exposure of internal fixation device after operation.
3. Occlusal relationship: Three months after the operation, the patient had no early occlusal contact, and the cusp staggered jaw had recovered.
4. Mouth opening: If the patient could open his or her mouth more than 3 cm at a follow-up visit 3 months after the operation, the patient's mouth opening was considered to have returned to normal.

If none of the above conditions occurred, the treatment was considered successful, with an excellent therapeutic effect. If less than or equal to two of the above conditions occurred without causing dysfunction, the therapeutic effect was considered to be satisfactory. If dysfunction or more than two of the above conditions occurred, the therapeutic effect was considered to be unsatisfactory. The Spearman

rank correlation coefficient was used to assess the effect of the operation and calculated using SPSS 23.0 (IBM Corp., Armonk, NY, USA). Differences were considered statistically significant if  $P < 0.05$ .

### 3. Results

There 26 patients were included in this study. After screening, 26 patients were included in this study, including 18 males and 8 females aged from 16 to 56 ( $35.92 \pm 12.88$ ) years. There were 15 cases of traffic accident injury and 8 cases of falling injury; the time to operation was 11 to 45 ( $24.62 \pm 12.38$ ) days. There were 15 cases (58%) of injury from traffic accidents, accounting for the vast majority of patients, 8 cases (30%) of injury from falling, and 3 cases (12%) of injury from falling objects. Among this cohort of 26 patients, the distribution of fractures was as follows: midfacial region fractures,  $n=11$  (43%); panfacial fractures,  $n=5$  (19%); basifacial region fractures,  $n=5$  (19%); and craniofacial fractures,  $n=5$  (19%). Patient data, other concomitant injuries, fracture characteristics, CT data and all complications are described in Table 1. A comparison of the therapeutic effects of the two surgical schemes is shown in Table 2.

In the treatment of panfacial fractures, the percentage of satisfactory results was 100% in group 1 and 0% in group 2, showing a dramatic difference (Table 1). The statistical results demonstrate that the use of a 3D-printed guide is relevant to the treatment result. The results in this study indicate dramatically improved treatment results from the combined use of CAN with 3D-printed models and guides compared to using CAN alone (Table 2). The operation time of the experimental group was significantly shorter than that of the control group (Table 3).

### 4. Discussion

Without 3D-printed models, reconstruction can be achieved by CAN with mirror image technology and virtual movement of fracture blocks, with improved surgical accuracy[18]. When double-sided and comminuted fractures occur, the healthy reference side is missing, and reconstruction with CAN is technologically impossible. In this study, a presurgical head model was 3D printed and artificially divided, followed by reconstruction into a postsurgical model. The postsurgical model was further scanned by CT and loaded into a CAN system. In this way, the reconstruction of multiple maxillofacial fractures was feasible by CAN.

Successful reconstruction from the combined use of CAN and 3D-printed guides further improves precision in the setting of reference points, clarification of the internal fixation point of the fracture end, and optimization of the surgical approach, all of which greatly contributes to the significantly improved treatment results in this study. The manner in which the combined use of the two technologies improves the three key components of surgical treatment and how they further lead to satisfactory treatment results are described in the following three paragraphs. This study showed that the combined use of the

two techniques significantly shortened the operation time, which is likely due to the fact that the intraoperative application of 3D guides and head molds can better address the above three problems (Table 3).

The setting of reference points is key for the successful treatment of maxillofacial fractures. When the occlusal relationship remains intact, the reference point can be set using the healthy side and fracture line[19]. However, the occlusal relationship and the healthy side are often missing in cases of multiple maxillofacial fractures, and the reference point cannot be restored by the use of CAN alone. Instead, the success of restoration can only be demonstrated after the surgery. This study shows that complete maxillary or mandibular dentition can be used as a reference point for fracture reduction in middle facial fractures, mandibular fractures and craniomaxillofacial fractures. Therefore, a reference point could be set without an occlusal guide, so there was no obvious difference in the treatment results between the experimental and control groups (Table 1). However, panfacial fractures were more complicated and challenging due to the loss of the healthy reference side and occlusal relationship, and the sole use of CAN was insufficient for treatment. Therefore, the combined use of the two technologies showed remarkable improvements in the treatment of panfacial fractures. In this study, the postoperative CT analysis showed that smaller difference in the bilateral G-K length than in the bilateral G-Er length, which is presumably attributed to the successful restoration of the occlusal relationship (Table 1). According to the above discussion, the precise setting of a reference point is crucial to the treatment of multiple maxillofacial fractures, and this can be achieved by the combined use of CAN and 3D-printed guides, as demonstrated in this study.

In addition to locating a reference point, the inability to determine the fixation position is another key limitation of CAN in the treatment of multiple maxillofacial fractures. This problem was also solved by the combined use of CAN and 3D printing. Research has indicated that the zygomatic sphenoid suture, maxillary alveolar arch, orbit, and orbital floor are key positions in facial fracture repair[20]. In this study, a head model of each patient was 3D-printed based on CT data to demonstrate the whole fracture in a straightforward manner. In this way, the optimal fixation point was easily determined. Preformed titanium plates were also created according to the 3D-printed model, which shortened the operation and improved the quality fit between the titanium plates and the bone surface[21, 22]. As a result, fracture segment displacement was avoided during and after the fixation process, and the probability of operation failure was subsequently reduced. Furthermore, the use of a preformed plate avoided repeated bending of the plate during the operation and reduced the risk of plate fracture after the treatment[23]. In this process, the fracture line was preliminarily fixed using the preformed titanium plate, and a retaining nail was implanted at both ends of the fracture line, followed by further inspection by CAN. Upon finishing this inspection, the titanium plate was successfully fixed.

Last, since CAN with a 3D-printed guide can be used to achieve precise localization and reconstruction, the physician can flexibly select and optimize the surgical approach, which can also greatly improve the treatment results[18]. In common maxillofacial treatment practice, a local incision is preferred over a coronal incision because it ensures exposure while minimizing trauma[24]. However, this approach is not feasible when comminuted fractures cover over 1/3 of the facial area because the fracture segments cannot be well exposed. As a result, insufficient fracture reduction may occur, leading to dislocated healing of the fracture. By using CAN alone, this tradeoff between the required exposure and size of the incision cannot be made, but with assistance from a 3D-printed guide, the problem can be solved. Although a coronal incision is commonly not preferred due to the large injury[25, 26], it was flexibly designed and adjusted in this study. The optimized surgical approach was selected based on the 3D-printed head model; thus, a small cut and sufficient exposure were both ensured. The surgical operation was also adjustable, allowing individualized treatment to be achieved. Additionally, when a 3D-printed guide was used together with CAN, the relative distance between the fracture end and the surgical scheme could be displayed on a screen in real time. The surgical field and application of local small incisions were expanded accordingly in fracture repair and reconstruction. As a result, the surgical trauma was minimized. According to our results, the rate of satisfactory results was 100% in group 1 (n=5) and 60% in group 2 (n=5). Compared with the results of common treatment practices involving a coronal incision, our results were much improved due to the combined use of CAN and 3D-printed guides (Table 2).

## 5. Conclusion

In conclusion, the combined use of CAN and 3D printing greatly mitigated the limitations of three key aspects in determining the treatment results: setting of the reference point, determination of the fixation position, and optimization of the surgical approach. Compared with the use of CAN alone, the combined use of the two technologies yielded greatly improved treatment results in this study, broadening our understanding of the treatment of multiple maxillofacial fractures.

## Declarations

### Funding

This work was supported by the Postgraduate Scientific Research Projects of Universities in Anhui Province (YJS20210306) and the Clinical Research Project of the First Affiliated Hospital of Anhui Medical University (LCJY2021YB001)

### Competing interests

The authors declare that they have no competing interests.

## Ethical approval

All human samples were collected with the patients' written informed consent and approval from the Institute Research Medical Ethics Committee of The First Affiliated Hospital of Anhui Medical University (Hefei, China).

## Patient consent

Written informed consent was obtained from all subjects for the publication of their data.

## Tables

Table 1. Fracture type of recruited patients and treatment results.

	Experimental Group	Control Group
Number of patients	13	13
Classification of fractures		
• Midfacial region fracture	6 (6, 0, 0)	5 (3, 1, 1)
• Basifacial region fracture	2 (2, 0, 0)	3 (2, 1, 0)
• Panfacial fracture	3 (2, 1, 0)	2 (0, 0, 2)
• Craniofacial fracture	2 (2, 0, 0)	3 (2, 1, 0)
Length of G-K (cm)		
• Left (mean)	5.36	5.4
• Right (mean)	5.39	5.35
Length of G-Er (cm)		
• Left (mean)	8.27	8.33
• Right (mean)	8.21	8.19
Complication		
• Infection	0	0
• Occlusal disorder	1	6
• Restricted mouth opening	0	1
• Midline displacement	1	2
• Bilateral asymmetry	0	3

[The treatment result was categorized as excellent, satisfactory, or unsatisfactory. The number indicates the number of patients in each category.]

**Table 2. Summary of treatment results**

	Therapeutic effect		
	Excellent	Satisfactory	Unsatisfactory
Experimental group	12	1	0
Control Group	7	3	3
$r_s$	0.448		
p	0.022		

Table 3. Comparison of operation time

	n	Operation time (min)
Experimental group	12	197.23±38.07
Control group	12	242.69±59.95
Z	-2.083	
p	0.037	

## References

- [1]. Zhou, H.H., et al., Clinical, retrospective case-control study on the mechanics of obstacle in mouth opening and malocclusion in patients with maxillofacial fractures. *Sci Rep*, 2018. 8(1): p. 7724.
- [2]. Ellis, E.R., A. El-Attar and K.F. Moos, An analysis of 2,067 cases of zygomatico-orbital fracture. *J Oral Maxillofac Surg*, 1985. 43(6): p. 417-28.
- [3]. Haworth, S., et al., A clinical decision rule to predict zygomatico-maxillary fractures. *J Craniomaxillofac Surg*, 2017. 45(8): p. 1333-1337.
- [4]. Kim, J.W., et al., The accuracy and stability of the maxillary position after orthognathic surgery using a novel computer-aided surgical simulation system. *BMC Oral Health*, 2019. 19(1): p. 18.
- [5]. Kim, J.W., et al., Computer-Aided Surgical Simulation for Yaw Control of the Mandibular Condyle and Its Actual Application to Orthognathic Surgery: A One-Year Follow-Up Study. *Int J Environ Res Public Health*, 2018. 15(11).
- [6]. Dupret-Bories, A., et al., Contribution of 3D printing to mandibular reconstruction after cancer. *Eur Ann Otorhinolaryngol Head Neck Dis*, 2018. 135(2): p. 133-136.
- [7]. Cheng, M., et al., Efficacy of surgical navigation in zygomaticomaxillary complex fractures: randomized controlled trial. *Int J Oral Maxillofac Surg*, 2021.
- [8]. Redua, R.B., et al., A complex orthognathic surgical approach correcting a Class III malocclusion involving traumatic dental injuries and a maxilla fracture. *Am J Orthod Dentofacial Orthop*, 2019. 155(5): p. 702-713.

- [9]. Cuellar, J., et al., Surgical or conservative treatment for mandibular condyle fractures. *Medwave*, 2018. 18(7): p. e7352.
- [10]. Sukegawa, S., T. Kanno and Y. Furuji, Application of computer-assisted navigation systems in oral and maxillofacial surgery. *Jpn Dent Sci Rev*, 2018. 54(3): p. 139-149.
- [11]. Bao, T., et al., Quantitative assessment of symmetry recovery in navigation-assisted surgical reduction of zygomaticomaxillary complex fractures. *J Craniomaxillofac Surg*, 2019. 47(2): p. 311-319.
- [12]. Sharma, A.P., et al., Management of Malocclusion after Maxillofacial Trauma. *Facial Plast Surg*, 2017. 33(6): p. 562-570.
- [13]. Kim, S.Y., Y.H. Choi and Y.K. Kim, Postoperative malocclusion after maxillofacial fracture management: a retrospective case study. *Maxillofac Plast Reconstr Surg*, 2018. 40(1): p. 27.
- [14]. Strong, E.B. and C. Gary, Management of Zygomaticomaxillary Complex Fractures. *Facial Plast Surg Clin North Am*, 2017. 25(4): p. 547-562.
- [15]. Yu, H., et al., The indication and application of computer-assisted navigation in oral and maxillofacial surgery-Shanghai's experience based on 104 cases. *J Craniomaxillofac Surg*, 2013. 41(8): p. 770-4.
- [16]. Chu, Y.Y., et al., Application of real-time surgical navigation for zygomatic fracture reduction and fixation. *J Plast Reconstr Aesthet Surg*, 2021.
- [17]. Yang, C., et al., Application of Computer-Assisted Navigation System in Acute Zygomatic Fractures. *Ann Plast Surg*, 2019. 82(1S Suppl 1): p. S53-S58.
- [18]. Udhay, P., et al., Computer-assisted navigation in orbitofacial surgery. *Indian J Ophthalmol*, 2019. 67(7): p. 995-1003.
- [19]. Tepper, O.M., et al., Use of virtual 3-dimensional surgery in post-traumatic craniomaxillofacial reconstruction. *J Oral Maxillofac Surg*, 2011. 69(3): p. 733-41.
- [20]. Curtis, W. and B.B. Horswell, Panfacial fractures: an approach to management. *Oral Maxillofac Surg Clin North Am*, 2013. 25(4): p. 649-60.
- [21]. Shen, Y., et al., Using computer simulation and stereomodel for accurate mandibular reconstruction with vascularized iliac crest flap. *Oral Surg Oral Med Oral Pathol Oral Radiol*, 2012. 114(2): p. 175-82.
- [22]. Ciocca, L., et al., A CAD/CAM-prototyped anatomical condylar prosthesis connected to a custom-made bone plate to support a fibula free flap. *Med Biol Eng Comput*, 2012. 50(7): p. 743-9.

- [23]. Ribeiro-Junior, P.D., et al., Mandibular angle fractures treated with a single miniplate without postoperative maxillomandibular fixation: A retrospective evaluation of 50 patients. *Cranio*, 2018. 36(4): p. 234-242.
- [24]. Asamura, S., et al., Treatment of orbital floor fracture using a periosteum-polymer complex. *J Craniomaxillofac Surg*, 2010. 38(3): p. 197-203.
- [25]. Frodel, J.L. and L.J. Marentette, The coronal approach. Anatomic and technical considerations and morbidity. *Arch Otolaryngol Head Neck Surg*, 1993. 119(2): p. 201-7; discussion 140.
- [26]. Yanan, W., et al., [Complications of supratemporalis approach with scalp coronal incision for orbital-zygomatic fracture]. *Hua Xi Kou Qiang Yi Xue Za Zhi*, 2017. 35(1): p. 73-76.

## Figures

**Figure 1**

Flowchart of the clinical trial

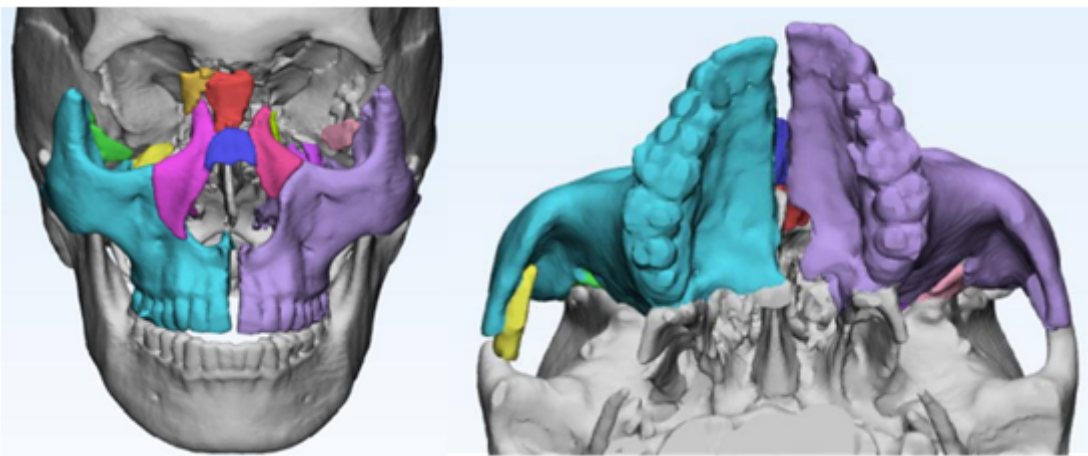


**Figure 2**

Establishment of a 3D model of the patient's maxillofacial region

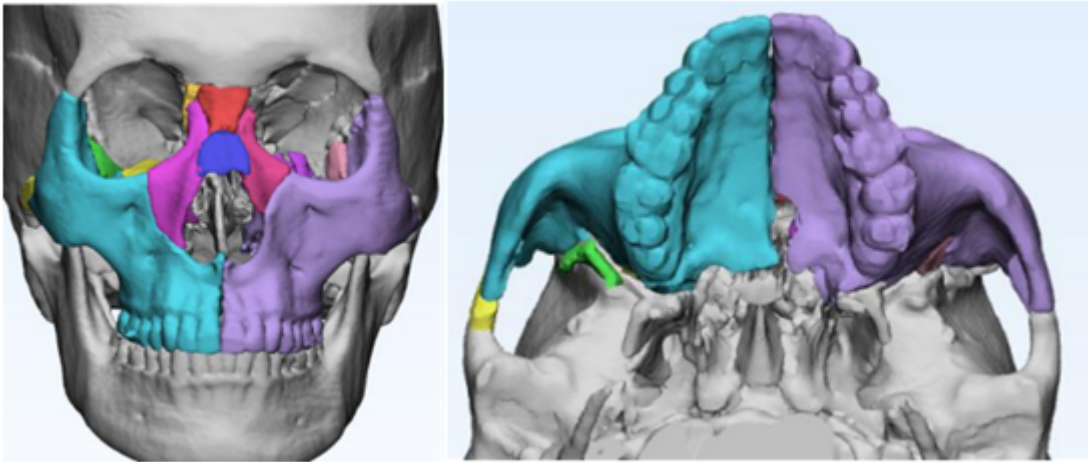


**Figure 3**

Establishment of a 3D model of the virtual surgery

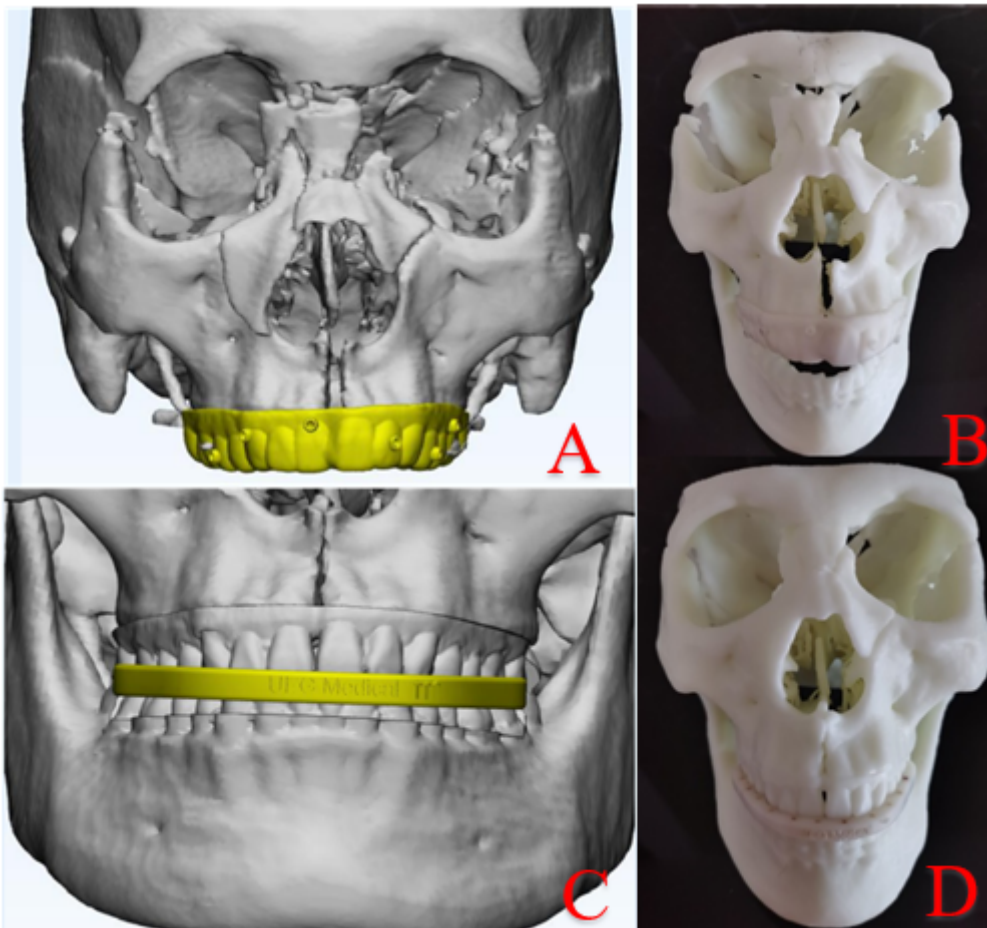


**Figure 4**

Design and manufacture of the 3D-printed guide plate and head mold. Design of the navigation registration guide (A), 3D-printed model of the patient's skull before surgery and registration guide for the

navigation system (B), design of the occlusal guide (C), and 3D-printed model of the skull after the virtual operation and insertion of the occlusal guide (D).

### **Figure 5**

Surgical operation. 3D-printed guide for assisting CAN registration (A), CAN for verification of the location of the fracture segment in real time (B), 3D-printed guide for guiding fracture segment reduction (C).

### **Figure 6**

CT images of a patient: Before surgery (A), after surgery (B).